Joint effects of genes underlying a temperature specialization tradeoff in yeast

Faisal AlZaben[1], Julie N. Chuong[1,2], Melanie B. Abrams[1], and Rachel B. Brem[1]

[1]Department of Plant and Microbial Biology, UC Berkeley, Berkeley, CA; [2]Ph.D. Program in Biology, New York University, New York, NY

Abstract

A central goal of evolutionary genetics is to understand, at the molecular level, how organisms adapt to their environments. Landmark work has characterized steric clashes between variants arising in a given protein as it evolves a new function. For many traits, any such single gene represents only part of a complex architecture, whose genetic mechanisms remain poorly understood. We studied the joint effect of eight genes underlying thermotolerance in *Saccharomyces cerevisiae,* when introduced into a thermosensitive species, *S. paradoxus*. The data revealed no sign epistasis: most gene combinations boosted thermotolerance, and none was deleterious. And the genes also governed a heretofore unknown advantage in cold growth by *S. paradoxus*. These results shed light on how and why thermotolerance arose in *S. cerevisiae*, and they suggest a paradigm in which, if protein repacking is a difficult step in adaptation, combining whole-gene modules may be far less constrained.

Author summary

The building of new traits by evolution can be difficult and slow. A given DNA variant may be the linchpin of a beneficial trait in some individuals and, in others, have the opposite effect—torpedo fitness altogether. Such effects have been best studied among amino acids in a given protein, whose changing side chains crowd each other unless they arise in a particular order. We set out to complement this literature by studying adaptive variants that are not in the same protein, but rather scattered across unlinked genes. We used as a model system eight genes that govern the ability of the unicellular yeast *Saccharomyces cerevisiae* to grow at high temperature. We introduced this suite of genes stepwise into a non-thermotolerant sister species, and found that the more *S. cerevisiae* loci we added, the better the phenotype. We saw no evidence for toxic interactions between the variant genes as they were combined. We also used the eight-fold transgenic to dissect the mechanism and the evolutionary forces underlying the thermotolerance trait. Together, our data suggest a principle for the field in which repacking a given protein is the hard part of evolution, and assembling combinations of unlinked loci is far easier.

Introduction

Understanding how organisms acquire new traits is a driving question in evolutionary biology. Many traits of particular interest are adaptations, meaning they promote fitness and have risen to high frequency in a population via positive selection. Genomic methods can pinpoint changes that underlie this process at the DNA level; gold-standard validation experiments will then test the impact of a given candidate locus by swapping alleles between taxa. Landmark findings have emerged from this approach, in adaptations from microbes to mammals (Savolainen et al., 2013; Weiss and Brem, 2019).

This literature, by necessity, tends to highlight the contribution of one model gene at a time to an adaptation, even if many other loci may also contribute (Castro et al., 2019; Chan et al., 2010; Kryazhimskiy et al., 2014; Linnen et al., 2013, 2009; Xie et al., 2019). For a complete picture of the complex genetic architecture of a trait, we would establish how the underlying genes work together, and how they were coordinated during evolution. In fact, analogous questions have found answers in the study of adaptive amino acid changes in a given protein, as combinations of these variants are introduced from one taxon into another (Anderson et al., 2016; Bridgham et al., 2009; Escudero et al., 2020; Finnigan et al., 2012; Lindsey et al., 2013; Liu et al., 2018; Palmer et al., 2015, 2015; Pillai et al., 2020; Toprak et al., 2011; Weinreich et al., 2006). Results have highlighted the role of sign epistasis, when a variant boosts fitness in some versions of the protein and confers a defect in others—requiring the suite of mutations to arise in a particular order to avoid deleterious effects (Starr and Thornton, 2016; Weinreich et al., 2005). Whether the multiple unlinked genes underlying a complex adaptation depend on each other to this degree is less well understood. Laboratory evolution has allowed genomic surveys (Blount et al., 2012; Good et al., 2017; Johnson et al., 2021; Kryazhimskiy et al., 2014) and, in some cases, experimental validation (Chou et al., 2011; Khan et al., 2011) of interactions between adaptive genes. Testing these principles in the context of evolution from the wild has posed a key challenge (although see Marcusson et al., 2009).

To help fill this analysis gap, we set out to use natural variation in *Saccharomyces* yeasts as a model. *S. cerevisiae* strains, from the wild and the lab, grow well up to 41°C. All other species in the *Saccharomyces* clade, whose common ancestor lived ~20 million years ago, grow poorly at high temperatures, though many outperform *S. cerevisiae* in the cold (Hittinger, 2013). In previous work we focused on thermotolerance as a case study of interspecies divergence (Weiss et al., 2018). We identified eight loci underlying the trait, using *S.*

paradoxus, the closest sister species to *S. cerevisiae,* as a representative of the inferred ancestral state. Derived, adaptive alleles of the mapped genes in *S. cerevisiae,* when tested individually for their marginal effects, were partially necessary or sufficient for thermotolerance, or both (Weiss et al., 2018). But how these genes work together has remained unknown. We thus aimed to investigate the joint effects of unlinked thermotolerance loci. And we expected that any answers could also help elucidate other facets of the mechanism and the evolutionary history of the thermotolerance trait.

Results

Combining thermotolerance loci to reconstitute a complex trait

Our previous screen uncovered pro-thermotolerance alleles in *S. cerevisiae* of the chromosome segregation/mitosis genes *DYN1, MYO1, SCC2, APC1,* and *ESP1*, and the transcription/translation genes *AFG2* and *TAF2* (Table 1; Weiss et al., 2018). To explore the joint function of these unlinked loci, we introduced the alleles of all eight from DVBPG1373, a soil isolate of *S. cerevisiae* from the Netherlands, into Z1, a strain of the sister species *S. paradoxus,* isolated from an English oak tree (Liti et al., 2009). Our approach used a stepwise set of gene replacements. With CRISPR/Cas9 we introduced the *S. cerevisiae* allele of the promoter and coding region of a given gene into the endogenous location in wild-type *S. paradoxus*; we used the resulting strain as a background for the replacement of the *S. paradoxus* allele of the next gene by that of *S. cerevisiae*; and so on until all eight genes were swapped into one genome (Figure 1, bottom).

We first assayed growth of the eight-gene transgenic and the wild-type parental species at 39°C, with biomass accumulation as a readout of strain performance. The results revealed an advantage of 1.98-fold attributable to the eight *S. cerevisiae* alleles in the *S. paradoxus* background (Figure 1 and Table S1A), with no such effect in 28°C control conditions (Figure S1). This contrasted with the <1.3-fold improvement in thermotolerance from any single *S. cerevisiae* gene, when swapped on its own into *S. paradoxus* (Figure 1 and Weiss et al., 2018).

That is, the impact of all eight *S. cerevisiae* loci together outstripped the marginal effect of any one locus, and came close to the maximum expectation under a model of additive gene function (8 x 30% = 2.4-fold improvement over *S. paradoxus* wild-type). This joint phenotype recapitulated 15% of the trait divergence between wild-type *S. cerevisiae* and *S. paradoxus* at 39°C (Figure 1), with comparable results at temperatures down to 37°C (Figure S2). These data make clear that the full genetic architecture of *S. cerevisiae* thermotolerance must involve more loci than the eight we have manipulated here—highlighting the potential for very high genetic complexity of this trait divergence between species.

No sign epistasis among thermotolerance loci

We next turned to the strains we had made in the service of the eight-gene thermotolerant transgenic. These harbored *S. cerevisiae* alleles of one thermotolerance gene in the *S. paradoxus* background, two genes, three genes, and so on (Figure 1, bottom). We considered this strain panel as an arbitrary trajectory through a gene-wise genetic landscape. In this scheme, the *S. cerevisiae* allele of each gene (including the promoter and coding region) would be a module gained in its entirety, in each step on a path from the *S. paradoxus* wild-type to the eight-locus swap. For each strain of the panel, we assayed biomass accumulation at 39°C. The results revealed a monotonic relationship between thermotolerance and the number of *S. cerevisiae* gene modules introduced into *S. paradoxus* (Figure 1), with no such trend in a 28°C control (Figure S1 and Table S1B). Most salient in the 39°C growth data was the absence of sign epistasis: many combinations of *S. cerevisiae* gene modules improved the ability to accumulate cell density, and no combinations had deleterious effects.

Inspecting our genotype-phenotype map in more detail, we noted that the simplest transgenic, bearing the *S. cerevisiae* allele of *DYN1* in the *S. paradoxus* background, had a phenotype that was indistinguishable from descendants also bearing *S. cerevisiae* alleles of *MYO1* and *SCC2* (Figure 1 and Table S1A). Thus the benefit of the latter genes, discernable when each was introduced on its own into *S. paradoxus* (Weiss et al., 2018), was either below our detection limit or absent altogether in combination with *S. cerevisiae DYN1*. In the later stages of the allele-swap trajectory, we noted stair-step increases in thermotolerance as we added the remaining *S. cerevisiae* alleles into *S. paradoxus,* reaching statistical significance in almost every case (Figure 1 and Table S1A). These results parallel the thermotolerance gains conferred by *S. cerevisiae* alleles of most

of our genes when tested independently in the wild-type species and in their hybrid (Weiss et al., 2018). Overall, our combinations of *S. cerevisiae* gene replacements into *S. paradoxus* can be summarized as yielding benefits without threatening fitness at high temperature, underscoring their evolvability in the backgrounds we have studied here.

Thermotolerance loci improve viability only during active growth

We next aimed to investigate cellular mechanisms of thermotolerance, using as a tool the strain with all eight of our focal genes from *S. cerevisiae* swapped into *S. paradoxus*. We focused on cell viability, as assayed by counts of colony forming units (CFUs) from aliquots of liquid culture at 39°C. In a first characterization of strain performance in growing cultures under this setup, *S. paradoxus* cells were much less viable than those of *S. cerevisiae,* across a range of warm temperatures (Figure S3), as expected (Weiss et al., 2018). We anticipated that *S. cerevisiae* alleles of our thermotolerance loci would rescue this phenotype, at least in part. This prediction bore out in our CFU assays from actively growing cultures: at 39°C, the eight-gene transgenic in the *S. paradoxus* background survived 7-fold better than did its *S. paradoxus* progenitor (Figure 2A). An analogous test of wild-type *S. cerevisiae* revealed three logs higher viability than that of *S. paradoxus* during active growth at 39°C (Figure 2A).

Interestingly, the defect of strains of *S. paradoxus* origin in the CFU assay (Figure 2A) was much bigger in magnitude than that seen in our measurements of biomass accumulation (Figure 1), in growing cultures. Such a discrepancy suggests that some cells with *S. paradoxus* genotypes manage to divide early in the heat treatment and then ultimately die, contributing at the end of the incubation to measured biomass but not viability. Qualitatively, however, both experiments led to the same conclusion: *S. cerevisiae* alleles of thermotolerance loci recapitulate part but not all of the advantage by *S. cerevisiae* relative to *S. paradoxus* during active growth at 39°C. As expected, we detected no viability differences between strains during active growth at 28°C (Figure S4A).

To gain insight into why *S. paradoxus* cells die at high temperature, we took account of the fact that all our thermotolerance genes encode housekeeping factors, most functioning in mitosis (Table 1). We hypothesized that failure of the *S. paradoxus* cell growth machinery was the proximal cause of death for this species at 39°C.

If so, we expected that the underlying alleles would not be a liability if cells did not enter the cell cycle in the first place. As a test of this notion, we retooled our viability assay to start by incubating a liquid culture at a permissive temperature until it reached stationary phase (when nutrients are exhausted and cell division arrests). We then switched these non-growing cultures to 39°C, and finally took aliquots for assays of CFUs. The results revealed that, when exposed to heat as a stationary-phase culture, *S. paradoxus* survived nearly as well as did *S. cerevisiae* (Figure 2B), in contrast to the many logs of difference between the species during active growth (Figure 2A). Likewise, transgenesis of our eight thermotolerance genes had no impact on high temperature survival in stationary phase (Figure 2B). Viability experiments on stationary-phase cultures at 28°C also found no difference between strains (Figure S4B).

These viability data show that the thermotolerance defect of *S. paradoxus* alleles from our eight-gene swap only manifests in actively growing cells. Such a finding dovetails with the hallmarks of cell cycle breakdown seen in microscopy assays of *S. paradoxus* at 39°C (Weiss et al., 2018). Together, our data support a model in which passage through mitosis itself is lethal at high temperature for *S. paradoxus*, whereas cells in an arrested state are protected from damage and death. *S. cerevisiae*, meanwhile, grows and divides successfully at 39°C, owing in part to its thermotolerant mitotic genes.

Antagonistic pleiotropy in tolerance of extreme temperatures

Given that *S. cerevisiae* is unique within its clade for its ability to grow at high temperatures, we anticipated that this trait could have evolved as part of a tradeoff. We considered that fitness in cold conditions would be a logical potential opposing character in such a scheme. Consistent with this picture, we observed generally better cold resistance across a panel of wild *S. paradoxus* isolates relative to wild *S. cerevisiae* (Figure S5). No such difference manifests at 28°C (Weiss et al., 2018). We reasoned that thermotolerance alleles at our eight focal genes could underlie, at least in part, the poor performance by *S. cerevisiae* in the cold. Indeed, our transgenic strain of the *S. paradoxus* background bearing thermotolerance genes from *S. cerevisiae* grew significantly worse than did wild-type *S. paradoxus* at 4°C (Figure 3). With respect to biomass accumulation, this strain recapitulated 15% of the divergence between the wild-type species at 4°C—paralleling the analogous quantity at 39°C (Figure 1). Indeed, given that the eight-gene swap had no defect at 28°C (Figure

S1) and a benefit at all warmer temperatures tested (Figures 1 and S2), we conclude that *S. cerevisiae* alleles at thermotolerance loci exhibit a cold-specific deleterious effect.

In viability assays during growth at 39°C, we had found robust differences in survival between *S. cerevisiae* and *S. paradoxus*, and survival effects of variation at our thermotolerance loci (Figure 2A). It remained an open question whether cold exposure would likewise drive cell death differently in different strains. In viability assays we saw very little difference between *S. cerevisiae*, *S. paradoxus*, and the eight-gene transgenic in the *S. paradoxus* background, in terms of CFUs after incubation at 4°C (Figure S6). This result underscores the difference in mechanism between cryotolerance and thermotolerance in this system, and establishes that *S. cerevisiae* alleles (at thermotolerance loci and others) slow growth in the cold rather than killing cells outright.

Discussion

As a field, genetics has made great strides in pinpointing the molecular basis of complex adaptations. But even in the best-characterized model systems, how the underlying genes evolve and function together has remained elusive. In this work, we have elucidated the joint effects of eight genes contributing to *S. cerevisiae* thermotolerance. Our findings shed light on how this species would have acquired its unique thermotolerance character, and what it would have given up in the process.

We found, when introducing *S. cerevisiae* thermotolerance genes into *S. paradoxus*, that no combination of these factors drove fitness down, and most had beneficial effects. This dovetails with comparable reports from laboratory evolution (Chou et al., 2011; Khan et al., 2011), in which unlinked adaptive loci together sometimes yielded an effect less than the sum of their parts (*i.e.*, were subject to negative epistasis), but they were never deleterious. By contrast, in studies of amino acid variants within a given protein, deleterious combinations of adaptive alleles (exhibiting sign epistasis) show up routinely (Starr and Thornton, 2016; Weinreich et al., 2005)—for example, when a new, bulky side chain clashes with an existing protein scaffold, unless a potentiating mutation has made room first. Such a clash represents a so-called fitness valley among the possible mutational paths from an unfit ancestor to a fit descendant, which slows the adaptive process (Lynch, 2010; Weinreich et al., 2006). The emergent picture is one in which repacking a given protein may be the hardest part of adaptation, and combining adaptive variants across unlinked loci would often be less

constrained (Toprak et al., 2011). If so, collecting easily evolvable variants in many genes—each, say, a regulatory change (Roop et al., 2016), or an amino acid variant that requires no compensation—would represent a particularly fast route to solve a complex evolutionary problem.

Our work has also shown that our eight focal genes recapitulate only a fraction of the thermotolerance trait. The complete architecture is likely far more complex: conceivably, *S. cerevisiae* could have built thermotolerance via changes at hundreds of genes, during its divergence from *S. paradoxus*. Furthermore, if many loci, each with fairly modest effects, do contribute to thermotolerance, a model of soft sweeps (Messer and Petrov, 2013) becomes plausible as its evolutionary origin. Here we would envision a pool of many thermotolerance alleles segregating in an ancient, recombining *S. cerevisiae* population, a subset of which would have been sufficient for the trait in any one individual. That said, our eight mapped genes share sequence, and phenotypic effect, across strains of *S. cerevisiae* (Weiss et al., 2018), suggestive of a fairly hard sweep at least at these loci. In either case, polygenicity of the yeast thermotolerance trait would echo the ample evidence for highly complex trait variation within a species (Boyle et al., 2017), and the hundreds of putatively beneficial variants seen in adapted genomes after experimental evolution (Good et al., 2017).

Despite having manipulated only a fraction of the genetic determinants of thermotolerance, we were able to achieve insight into the mechanisms of the trait as well as its evolutionary history. Our discovery of a defect in the cold in *S. cerevisiae*, relative to *S. paradoxus*, complements previous temperature profiling using other assays across the genus (Hittinger, 2013; Salvadó et al., 2011). And we were able to pinpoint the genetic basis of this phenotype, at least in part, to pro-thermotolerance *S. cerevisiae* alleles at our focal genes. Since the latter exhibit signatures of positive selection in the wild in *S. cerevisiae* strains (Weiss et al., 2018), the emerging picture is one in which this species adapted to, and became a specialist in, warm environments, losing the putatively ancestral capacity to deal with cold. *S. cerevisiae* is thought to have originated in subtropical East Asia (Peter et al., 2018); it is thus tempting to speculate that hot ambient temperatures in these niches were an ecological driver of the changes we study here.

In summary, our data have suggested principles by which unlinked adaptive variants from the wild work together to exert their phenotypes. And with the joint effects of many loci taken into account, we have

uncovered a heretofore unknown evolutionary tradeoff. Given that naturally varying traits can be dissected in many organismal systems, including long-divergent species (Weiss and Brem, 2019), future pursuit of these trends more broadly will be well within reach.

Acknowledgements

The authors thank Dmitri Petrov for motivating the analysis of the thermotolerance of stationary-phase cultures; Abel Duarte for direction and advice with molecular biology; and Carly Weiss and Jeremy Roop for other helpful discussions.

Methods

Strain construction

Strains used in this work are listed in Table S2. To study combinations of *S. cerevisiae* alleles in an *S. paradoxus* background, we used as the latter the wild-type homozygous diploid *S. paradoxus* Z1, originally isolated from tree bark in the UK (Liti et al., 2009). We used our CRISPR/Cas9 method (Weiss et al., 2018), essentially as described but with slight modifications detailed below, to replace both copies of a given thermotolerance locus, at the endogenous location, with the allele from *S. cerevisiae* DBVPG1373, a soil isolate from the Netherlands (Liti et al., 2009). To build the eight-gene transgenic, we started with the single-gene transgenic in the Z1 background harboring the *S. cerevisiae* allele of *DYN1* from Weiss et al., 2018. We introduced *S. cerevisiae* alleles at additional genes in an iterative series of transformations; after each, we cultured an isogenic stock from a single colony for Sanger sequence confirmation and storage, and, where appropriate, we used this stock as input into the next transformation.

A given transformation involved donor DNA and constructs encoding guide RNAs for Cas9 to target replacement of the *S. paradoxus* allele with that from *S. cerevisiae* at either one or two loci, which Sanger sequencing then verified to be successful at one or both. For each locus we used designs of guide RNAs from Weiss et al., 2018 that targeted, for double-strand breaks, the endogenous Z1 allele by Cas9; one guide targeted a site ~1000bp upstream of the coding start of the gene of interest (or the 3' end of the closest upstream gene) in the Z1 genome and the other guide targeted a site near the coding stop. Cas9 editing

proceeded as described (Weiss et al., 2018). Briefly, for each transformation step of strain construction, one or two guide RNA pairs, targeting one or two loci respectively, were cloned into plasmid pBC712, which also encodes *Streptococcus pyogenes* Cas9. Next, DNA to serve as a repair template was generated for each relevant locus, via PCR from *S. cerevisiae* DBVPG1373, with 90bp primers that contained 70bp of sequence homologous to *S. paradoxus* Z1 on each side of the amplified DNA product. Finally, plasmid and repair template were transformed into the Z1 descendant as described (Weiss et al., 2018) at a ratio of 0.3 to 3.5 based on the length of the donor DNA, equivalent to 10^{12} dsDNA molecules for 10μg of plasmid. Putative transformants were purified and sequence-verified.

Growth assays

Measurements of biomass accumulation (growth efficiency) at 39°C in Figure 1 were done essentially as described (Weiss et al., 2018) with minor modifications. Briefly, for a given day's worth of experiments, wild-type *S. paradoxus* Z1 and one or more other strains of interest were streaked onto a yeast peptone dextrose (YPD) plate from a -80°C freezer stock and incubated at 28°C for 2 days. 2-8 colonies of a given strain were each inoculated in 5mL of liquid YPD and grown for 24 hours at 28°C with shaking at 200rpm to saturation; we refer to the cultures at this stage as pre-cultures. Each such replicate pre-culture was back-diluted into 10mL of YPD to achieve an OD_{600} of 0.05; incubated at 28°C until it reached an OD_{600} of 0.4-0.8; back-diluted again to OD_{600} of to achieve an OD_{600} of 0.1; and then incubated for 24 hours at 39°C. We tabulated the difference in OD_{600} between the final and initial timepoints across this 24-hour incubation for each culture. This procedure, from streaking on solid medium through inoculation, heat treatment, and biomass measurement, was repeated at least four times for each strain in the analysis of Figure 1. The resulting vector of biomass measurements across all replicates from all days for each strain was compared to that for each other strain with a one-tailed Mann-Whitney U test in Table S1.

Measurements of biomass accumulation at 28°C in Figure S1 were done as described (Weiss et al., 2018). Briefly, strains were streaked on solid plates and one colony per strain was pre-cultured in liquid at 28°C as above. Each such saturated pre-culture was back-diluted to achieve an OD_{600} of 0.05 and grown for an additional 5.5 hours at 28°C until it reached logarithmic phase. We transferred cells from each such pre-

culture, and YPD, to five replicate wells of a 96-well plate, with volumes sufficient to yield a total volume of 150 µL per well at an OD_{600} of 0.02. The plate was covered with a gas-permeable membrane (Sigma) and incubated with orbital shaking in an M200 plate reader (Tecan, Inc.) at 28°C for 24 hours. We tabulated the difference in OD_{600} between the final and initial timepoints across this 24-hour incubation for each replicate culture. The vector of these replicate measurements for each strain was compared to that from *S. paradoxus* with a two-tailed Mann-Whitney U test.

For measurements of biomass accumulation at 37°C - 39°C in Figure S2, strains were streaked, and three colonies of a given strain were pre-cultured in liquid as above. Each such replicate liquid culture was back-diluted into 10mL of YPD to achieve an OD_{600} of 0.05; incubated at 28°C until it reached an OD_{600} of 0.4-0.8; back-diluted again to OD_{600} of to achieve an OD_{600} of 0.1; and then incubated for 24 hours at the temperature of interest. We tabulated the difference in OD_{600} between the final and initial timepoints across this 24-hour incubation for each replicate culture. The vector of these replicate measurements for each strain at a given temperature was compared to that from *S. paradoxus* with a one-tailed Mann-Whitney U test. In Figure S2, lines are the result of a polynomial regression on the points, created using Seaborn's regplot in Python 3.7.

For measurements of growth at 4°C in Figure 3 and Figure S5, strains were streaked on solid plates and three or eight colonies per genotype, respectively, were pre-cultured in liquid as above. After the second back-dilution, each liquid culture was incubated for 11 days at 4°C in a rotating shaker at maximum speed in a cold room. The OD_{600} was measured on days 0, 4, 5, 7, 8, 9, 10, and 11, as well as on day 6 for the strains in Figure S5. To measure biomass accumulation (growth efficiency) we tabulated the difference in OD_{600} between the final and initial timepoints across this 11-day incubation for each replicate. We compared the vector of these replicate measurements for each strain against that from *S. paradoxus* with a one-tailed Mann-Whitney U test. Separately, we fit a logistic curve to the timecourse measurements for each replicate using Scipy's curve_fit function as a part of Scipy's optimize package (Python 3.7). Bounds for the parameters of the logistic equation (the carrying capacity, growth rate, and time to half-maximal growth) were constrained to the range -1.0 to 10.0, and the Trust Region Reflective algorithm was used to find the best fit. The vector of growth rate estimates across replicates for a given strain was compared to that from *S. paradoxus* with a one-tailed Mann-Whitney U test.

Viability assays

For the survey of viability phenotypes at high temperatures across wild-type isolates in Figure S3, strains were streaked out and four colonies of each were pre-cultured in liquid as for 39°C growth above, except that the initial pre-culture to achieve saturation lasted 48 hours. Each pre-culture was back-diluted into 10mL of YPD to reach an OD_{600} of 0.05 and then cultured for 24 hours at the temperature of interest (35°C - 38°C). The OD_{600} at the end of this timecourse was measured for each such replicate culture. Then to measure viability for each, we carried out a spotting assay, diluting aliquots from the culture in a 1:10 series and spotting 3µL of each dilution for growth on a solid YPD plate. After incubation at 28°C for two days, we used the dilution corresponding to the most dense spot that was not a lawn for the final report of viability: we counted the number of colonies in each of the two technical replicate spots, formulated the number of colony forming units per mL of undiluted culture (CFU/mL), and divided this ratio by the OD_{600} we had measured at the end of the liquid timecourse, to account for differences in the number of dead cells that contribute to the latter. At a given temperature, the vector of viability measurements across all replicate liquid cultures for all *S. cerevisiae* strains was compared to that for all *S. paradoxus* strains with a one-tailed Mann-Whitney U test.

For the comparison of viability between strains during log-phase growth at 39°C in Figure 2A, strains were streaked out and three colonies of each were pre-cultured at 28°C, back-diluted, and cultured at 39°C, as for the 39°C growth assays above. After 24 hours of incubation at 39°C, for each such replicate culture, spotting of dilutions and colony counting to yield CFU/mL/OD_{600} for each replicate liquid culture was done as above, except that we used two technical replicate spotting assay replicates for each culture, taking the average across them as the final report of viability. The vector of these viability measurements across replicates for a given strain was compared to that from *S. paradoxus* with a one-tailed Mann-Whitney U test.

For the comparison of viability between strains in stationary phase at 39°C in Figure 2B, strains were streaked out and three colonies of each were pre-cultured at 28° as for the 39°C growth assays above, except that that the initial pre-culture to achieve saturation lasted 72 hours. Each such replicate culture was then incubated (without back-dilution) at 39°C for 24 hours, after which spotting, colony counting, and statistical testing were as for Figure 2A.

For the comparison of viability between strains during log-phase growth at 28°C in Figure S4A, strains were streaked out and four colonies of each were pre-cultured at 28°C and back-diluted as for the 39°C growth assays above; each back-diluted replicate culture was incubated at 28°C for 24 hours, after which spotting and colony counting was as above. For the comparison of viability between strains in stationary phase at 28°C in Figure S4B, strains were streaked out as above, and three colonies of each were inoculated into liquid YPD at 28°C and incubated for 96 hours, after which spotting, colony counting, and statistical testing were as for Figure 2A.

For the comparison of viability between wild strains during log-phase growth at 4°C (Figure S6), aliquots from cultures set up for cold growth assays (see above) were taken at day 8 of the cold timecourse for spotting, colony counting, and statistical testing as for Figure 2A.

Gene	GO terms	Location	Description
AFG2 (YLR397C)	ribosomal large subunit biogenesis	Ch. XII 912550 - 914892	Essential for pre-60S maturation and release of several pre-ribosome maturation factors
APC1 (YNL172W)	mitotic cell cycle	Ch. XIV 310636 - 315882	Largest subunit of the Anaphase-Promoting Complex; a ubiquitin-protein ligase required for degradation of anaphase inhibitors
CEP3 (YMR168C)	mitotic cell cycle	Ch. XIII 597332 - 599158	Essential kinetochore protein; component of the CBF3 complex that binds the CDEIII region of the centromere
DYN1 (YKR054C)	mitotic cell cycle	Ch. XI 535647 - 547925	Heavy chain dynein; microtubule motor protein; required for anaphase spindle elongation
ESP1 (YGR098C)	mitotic cell cycle	Ch. VII 682566 - 687458	Separase/separin; aids in the dislocation of cohesin from chromatin and sister chromatin segregation.
MYO1 (YHR023W)	mitotic cell cycle	Ch. VIII 151666 - 157452	Type II myosin heavy chain; required for cytokinesis and cell separation
SCC2 (YDR180W)	mitotic cell cycle	Ch. IV 821295 - 825776	A complex required for loading of cohesin complexes onto chromosomes; involved in establishing sister chromatid cohesion during DSB repair via histone H2AX; subunit of cohesin loading factor (Scc2p-Scc4p)
TAF2 (YCR042C)	chromatin binding	Ch. III 201174 - 205397	TFIID subunit; involved in RNA polymerase II transcription initiaition

Table 1. Thermotolerance gene names and functions. GO, Gene Ontology biological process.

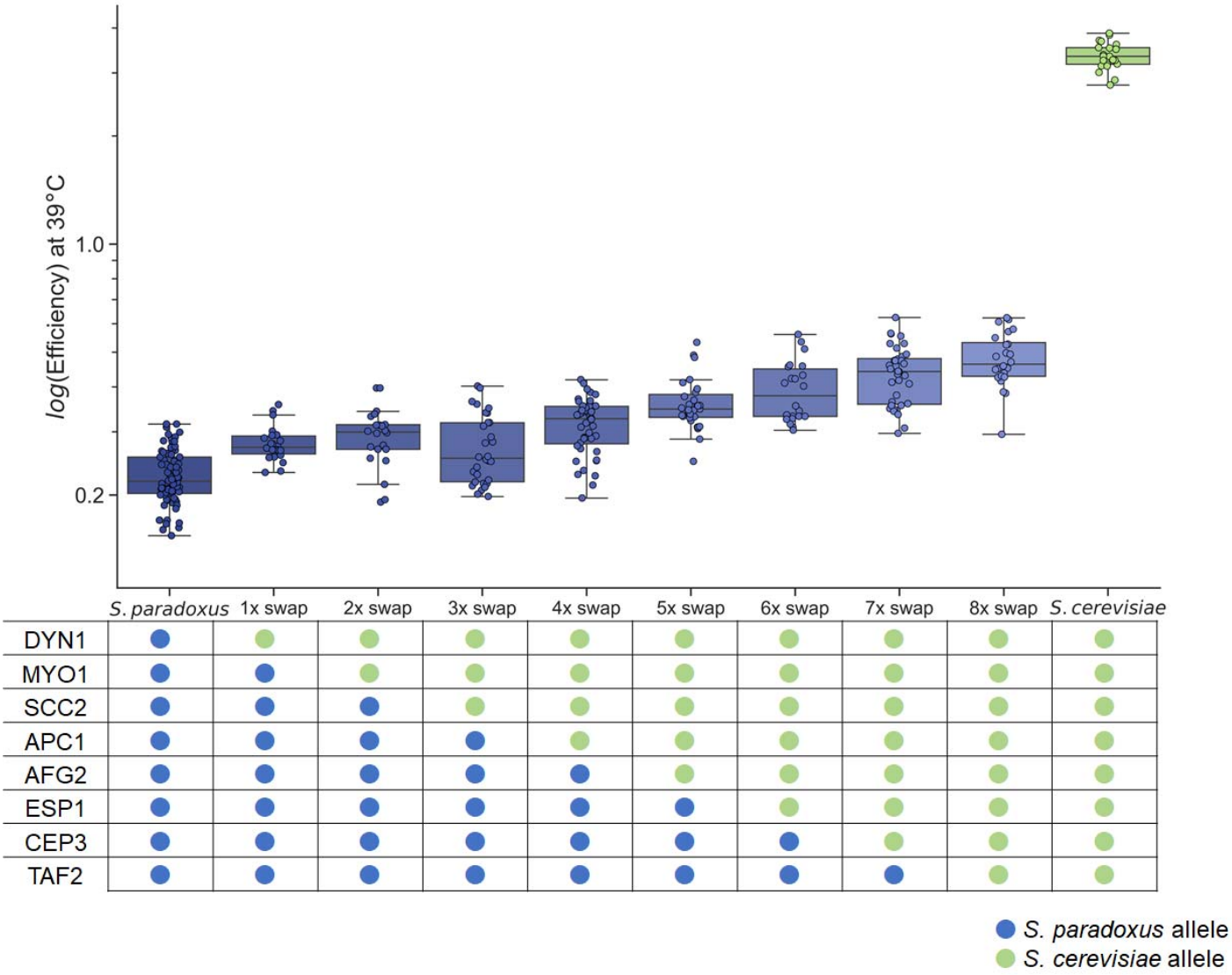

Figure 1. *S. cerevisiae* alleles of thermotolerance loci improve growth at high temperature. At top, the *y*-axis reports growth efficiency, the cell density after a 24-hour incubation at 39°C as a difference from the starting density. Each column reports data from the indicated wild-type species, or a transgenic *S. paradoxus*

strain harboring *S. cerevisiae* alleles of the indicated thermotolerance loci. Points report individual biological replicates. Boxes show the median and span the interquartile range of the data (IQR, 25%-75%); whiskers are 1.5 times the interquartile range, and do not report outliers. Statistical analyses are reported in Table S1A. At bottom, each cell reports the genotype at the indicated locus in the indicated strain.

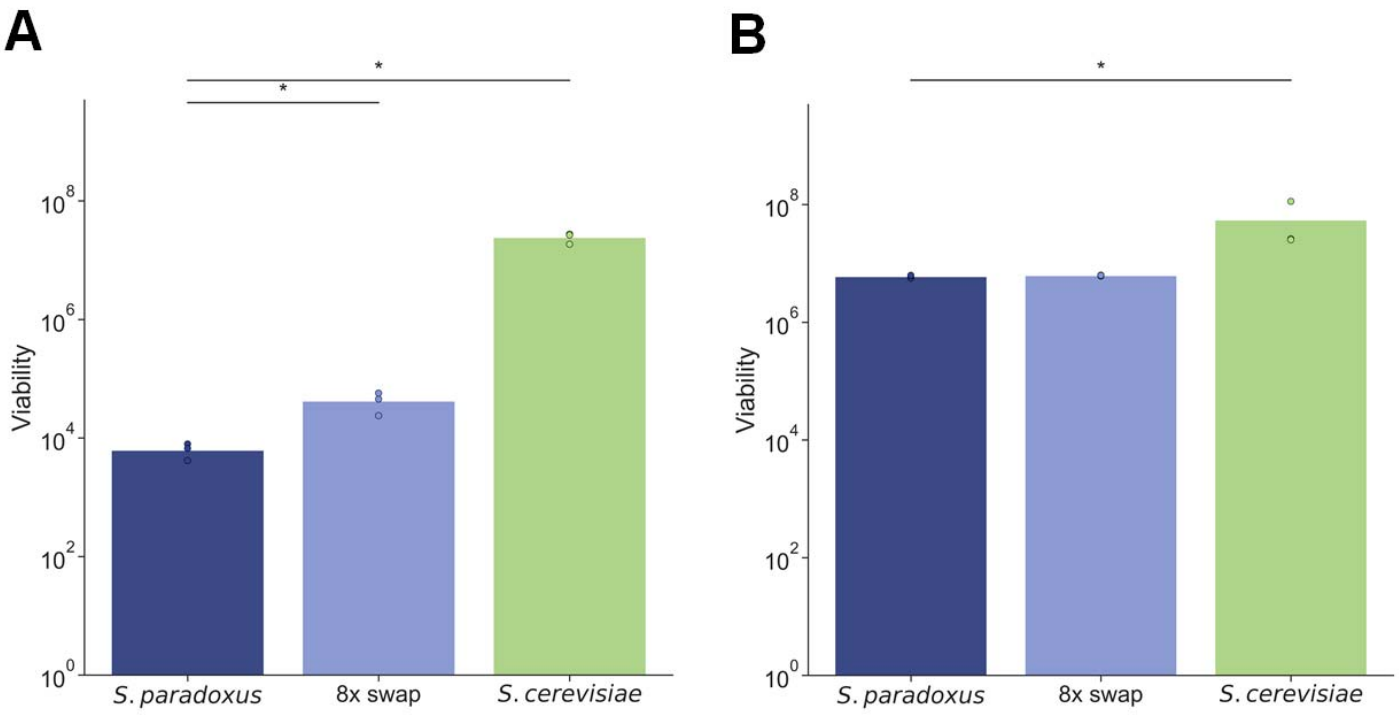

Figure 2. *S. cerevisiae* alleles of thermotolerance loci improve heat survival during growth but not in stationary phase. In a given panel, each column reports viability after heat treatment of the wild-type of the indicated species, or the *S. paradoxus* strain harboring eight thermotolerance loci from *S. cerevisiae* (8x swap). The *y*-axis reports the number of colonies formed on solid medium from 1 mL of heat-treated liquid culture in (A) logarithmic growth or (B) stationary phase, normalized by turbidity. Points and bar heights report individual biological replicates and their means, respectively. *, Mann-Whitney U $p \leq 0.05$.

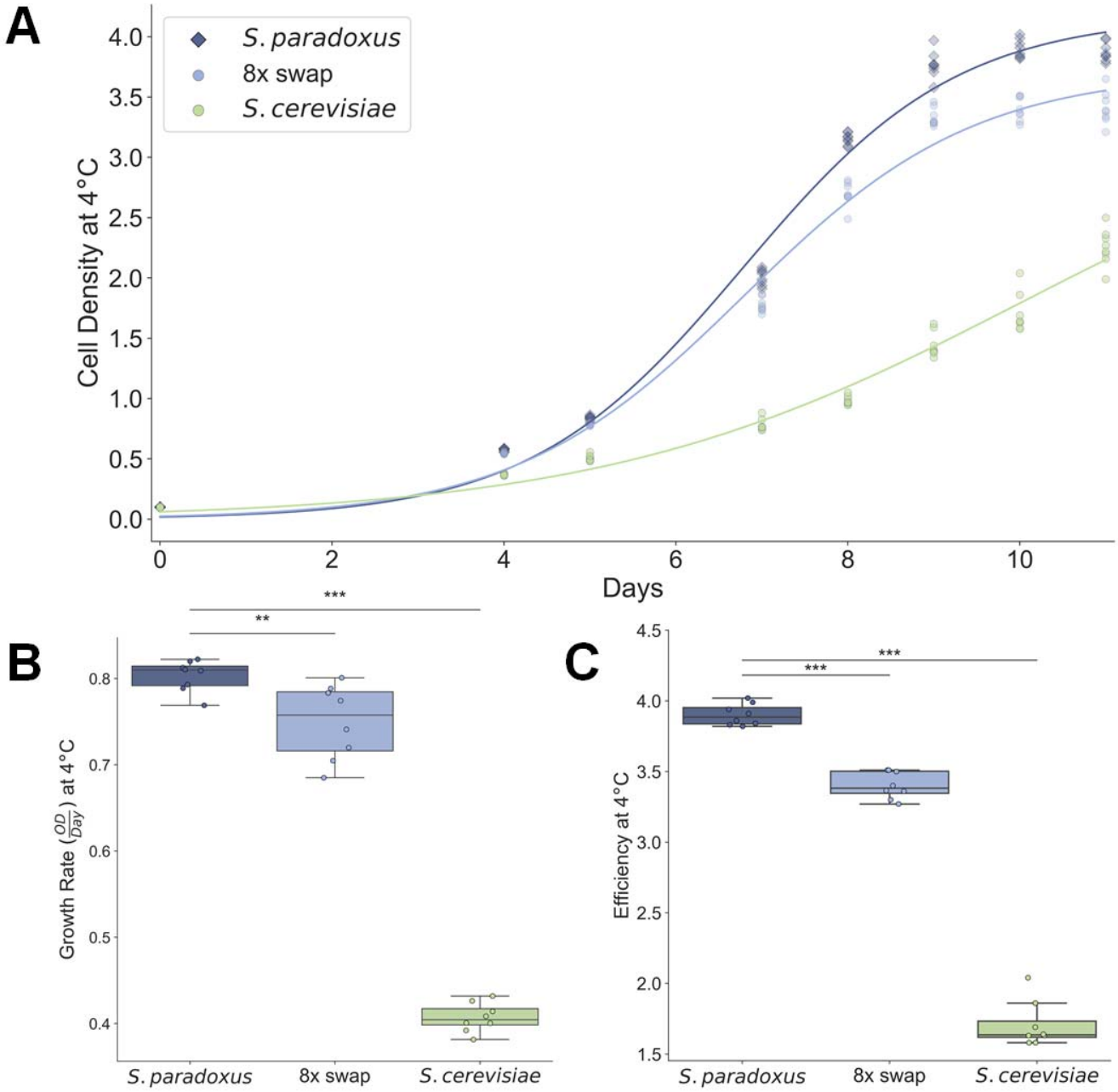

Figure 3. *S. cerevisiae* alleles of thermotolerance loci compromise growth in the cold. (A) Each trace reports a timecourse of growth at 4°C of the wild-type of the indicated species, or the *S. paradoxus* strain harboring eight thermotolerance loci from *S. cerevisiae* (8x swap). For a given strain, points on a given day report biological replicates; lines report the average fit from a logistic regression across replicates. (B) The *y*-axis reports growth rate, in units of cell density (optical density, OD) per day, from the average logistic fit of the

timecourse in (A) for the indicated strain. (C) The *y*-axis reports, for day 10 of the timecourse in (A) for the indicated strain, growth efficiency, the cell density after a 10-day incubation at 4°C as a difference from the starting density. In (B) and (C), points report individual biological replicates. Boxes show the median and span the interquartile range of the data (IQR, 25%-75%); whiskers are 1.5 times the interquartile range, and do not report outliers. ** and ***, Mann-Whitney U $p \leq 0.004$ and $p \leq 0.0005$, respectively.

References

1. Linnen CR, Poh Y-P, Peterson BK, Barrett RDH, Larson JG, Jensen JD, et al. Adaptive evolution of multiple traits through multiple mutations at a single gene. Science. 2013;339: 1312–1316. doi:10.1126/science.1233213

2. Chan YF, Marks ME, Jones FC, Villarreal G, Shapiro MD, Brady SD, et al. Adaptive evolution of pelvic reduction in sticklebacks by recurrent deletion of a Pitx1 enhancer. Science. 2010;327: 302–305. doi:10.1126/science.1182213

3. Bridgham JT, Ortlund EA, Thornton JW. An epistatic ratchet constrains the direction of glucocorticoid receptor evolution. Nature. 2009;461: 515–519. doi:10.1038/nature08249

4. Boyle EA, Li YI, Pritchard JK. An Expanded View of Complex Traits: From Polygenic to Omnigenic. Cell. 2017;169: 1177–1186. doi:10.1016/j.cell.2017.05.038

5. Castro JP, Yancoskie MN, Marchini M, Belohlavy S, Hiramatsu L, Kučka M, et al. An integrative genomic analysis of the Longshanks selection experiment for longer limbs in mice. Elife. 2019;8. doi:10.7554/eLife.42014

6. Liu Q, Onal P, Datta RR, Rogers JM, Schmidt-Ott U, Bulyk ML, et al. Ancient mechanisms for the evolution of the bicoid homeodomain's function in fly development. Elife. 2018;7. doi:10.7554/eLife.34594

7. Weinreich DM, Delaney NF, Depristo MA, Hartl DL. Darwinian evolution can follow only very few mutational paths to fitter proteins. Science. 2006;312: 111–114. doi:10.1126/science.1123539

8. Palmer AC, Toprak E, Baym M, Kim S, Veres A, Bershtein S, et al. Delayed commitment to evolutionary fate in antibiotic resistance fitness landscapes. Nat Commun. 2015;6: 7385. doi:10.1038/ncomms8385

9. Chou H-H, Chiu H-C, Delaney NF, Segrè D, Marx CJ. Diminishing returns epistasis among beneficial mutations decelerates adaptation. Science. 2011;332: 1190–1192. doi:10.1126/science.1203799

10. Weiss CV, Brem RB. Dissecting Trait Variation across Species Barriers. Trends Ecol Evol. 2019;34: 1131–1136. doi:10.1016/j.tree.2019.07.013

11. Xie KT, Wang G, Thompson AC, Wucherpfennig JI, Reimchen TE, MacColl ADC, et al. DNA fragility in the parallel evolution of pelvic reduction in stickleback fish. Science. 2019;363: 81–84. doi:10.1126/science.aan1425

12. Savolainen O, Lascoux M, Merilä J. Ecological genomics of local adaptation. Nat Rev Genet. 2013;14: 807–820. doi:10.1038/nrg3522

13. Okada Y. Effects of isoproterenol on chemical carcinogenesis with DMBA in mouse salivary glands. J Oral Pathol. 1979;8: 340–350. doi:10.1111/j.1600-0714.1979.tb01837.x

14. Lofgren DL, Stewart TS. Efficacy of alternative multivariate best linear unbiased prediction models for genetic evaluation of swine. J Anim Sci. 1991;69: 4388–4396. doi:10.2527/1991.69114388x

15. Starr TN, Thornton JW. Epistasis in protein evolution. Protein Sci. 2016;25: 1204–1218. doi:10.1002/pro.2897

16. Anderson DP, Whitney DS, Hanson-Smith V, Woznica A, Campodonico-Burnett W, Volkman BF, et al. Evolution of an ancient protein function involved in organized multicellularity in animals. Elife. 2016;5: e10147. doi:10.7554/eLife.10147

17. Finnigan GC, Hanson-Smith V, Stevens TH, Thornton JW. Evolution of increased complexity in a molecular machine. Nature. 2012;481: 360–364. doi:10.1038/nature10724

18. Toprak E, Veres A, Michel J-B, Chait R, Hartl DL, Kishony R. Evolutionary paths to antibiotic resistance

under dynamically sustained drug selection. Nat Genet. 2011;44: 101–105. doi:10.1038/ng.1034

19. Lindsey HA, Gallie J, Taylor S, Kerr B. Evolutionary rescue from extinction is contingent on a lower rate of environmental change. Nature. 2013;494: 463–467. doi:10.1038/nature11879

20. Weiss CV, Roop JI, Hackley RK, Chuong JN, Grigoriev IV, Arkin AP, et al. Genetic dissection of interspecific differences in yeast thermotolerance. Nat Genet. 2018;50: 1501–1504. doi:10.1038/s41588-018-0243-4

21. Peter J, De Chiara M, Friedrich A, Yue J-X, Pflieger D, Bergström A, et al. Genome evolution across 1,011 Saccharomyces cerevisiae isolates. Nature. 2018;556: 339–344. doi:10.1038/s41586-018-0030-5

22. Blount ZD, Barrick JE, Davidson CJ, Lenski RE. Genomic analysis of a key innovation in an experimental Escherichia coli population. Nature. 2012;489: 513–518. doi:10.1038/nature11514

23. Will JL, Kim HS, Clarke J, Painter JC, Fay JC, Gasch AP. Incipient balancing selection through adaptive loss of aquaporins in natural Saccharomyces cerevisiae populations. PLoS Genet. 2010;6: e1000893. doi:10.1371/journal.pgen.1000893

24. Marcusson LL, Frimodt-Møller N, Hughes D. Interplay in the selection of fluoroquinolone resistance and bacterial fitness. PLoS Pathog. 2009;5: e1000541. doi:10.1371/journal.ppat.1000541

25. Kryazhimskiy S, Rice DP, Jerison ER, Desai MM. Microbial evolution. Global epistasis makes adaptation predictable despite sequence-level stochasticity. Science. 2014;344: 1519–1522. doi:10.1126/science.1250939

26. Khan AI, Dinh DM, Schneider D, Lenski RE, Cooper TF. Negative epistasis between beneficial mutations in an evolving bacterial population. Science. 2011;332: 1193–1196. doi:10.1126/science.1203801

27. Linnen CR, Kingsley EP, Jensen JD, Hoekstra HE. On the origin and spread of an adaptive allele in deer

mice. Science. 2009;325: 1095–1098. doi:10.1126/science.1175826

28. Pillai AS, Chandler SA, Liu Y, Signore AV, Cortez-Romero CR, Benesch JLP, et al. Origin of complexity in haemoglobin evolution. Nature. 2020;581: 480–485. doi:10.1038/s41586-020-2292-y

29. Weinreich DM, Watson RA, Chao L. Perspective: Sign epistasis and genetic constraint on evolutionary trajectories. Evolution. 2005;59: 1165–1174.

30. Johnson MS, Gopalakrishnan S, Goyal J, Dillingham ME, Bakerlee CW, Humphrey PT, et al. Phenotypic and molecular evolution across 10,000 generations in laboratory budding yeast populations. eLife. 2021;10: e63910. doi:10.7554/eLife.63910

31. Roop JI, Chang KC, Brem RB. Polygenic evolution of a sugar specialization trade-off in yeast. Nature. 2016;530: 336–339. doi:10.1038/nature16938

32. Liti G, Carter DM, Moses AM, Warringer J, Parts L, James SA, et al. Population genomics of domestic and wild yeasts. Nature. 2009;458: 337–341. doi:10.1038/nature07743

33. Messer PW, Petrov DA. Population genomics of rapid adaptation by soft selective sweeps. Trends Ecol Evol. 2013;28: 659–669. doi:10.1016/j.tree.2013.08.003

34. Escudero JA, Nivina A, Kemble HE, Loot C, Tenaillon O, Mazel D. Primary and promiscuous functions coexist during evolutionary innovation through whole protein domain acquisitions. Elife. 2020;9. doi:10.7554/eLife.58061

35. Hittinger CT. Saccharomyces diversity and evolution: a budding model genus. Trends Genet. 2013;29: 309–317. doi:10.1016/j.tig.2013.01.002

36. Lynch M. Scaling expectations for the time to establishment of complex adaptations. Proc Natl Acad Sci U S A. 2010;107: 16577–16582. doi:10.1073/pnas.1010836107

37. Salvadó Z, Arroyo-López FN, Guillamón JM, Salazar G, Querol A, Barrio E. Temperature adaptation markedly determines evolution within the genus Saccharomyces. Appl Environ Microbiol. 2011;77: 2292–2302. doi:10.1128/AEM.01861-10

38. Good BH, McDonald MJ, Barrick JE, Lenski RE, Desai MM. The dynamics of molecular evolution over 60,000 generations. Nature. 2017;551: 45–50. doi:10.1038/nature24287